Spring 5-9-2020

Sexually Dimorphic Alterations in Brain Morphology of Astrocyte Conditional System xc- Knockout Mice

Gabrielle Emily Samulewicz

Sexually Dimorphic Alterations in Brain Morphology of Astrocyte Conditional System x_c^- Knockout Mice

A Thesis Submitted in Partial Fulfillment of the
Requirements of the Renée Crown University Honors Program at
Syracuse University

Gabrielle Samulewicz

Candidate for Bachelor of Science
and Renée Crown University Honors
Spring 2020

Honors Thesis in Your Major

Thesis Advisor: _____
Dr. Sandra J. Hewett

Thesis Reader: _____
Dr. Jessica MacDonald

Honors Director: _____
Dr. Danielle Smith, Director

Abstract

Astrocytes play a vital role in orchestrating the precise brain wiring that occurs during development and are essential for maintaining homeostasis into adulthood. The cystine/glutamate antiporter, system x_c^-, in the central nervous system is especially abundant in astrocytes and itself is known to contribute importantly to the basal extracellular glutamate concentration as well as the intracellular and extracellular glutathione levels, either of which, if perturbed, could alter brain development and/or contribute to degeneration. Thus, to determine whether loss of astrocyte system x_c^- might alter brain morphology, I studied a conditional astrocyte system x_c^- knockout mouse (AcKO). Tissue was harvested from male and female mice and gross morphological measurements over the rostro-caudal extent of each brain were made of the cerebral hemispheres, cortex, hippocampus, striatum, lateral ventricles, and corpus callosum. The following sex and genotype differences were observed. In female mice, corpus callosal area in AcKO mice was significantly larger and lateral ventricular area significantly smaller than sex-matched wild-type littermate controls. In males, lateral ventricular area was also smaller in AcKO mice and this occurred in association with a significantly larger striatal area than sex-matched littermate controls. Both male and female AcKO mice had larger hippocampal areas than their wild-type controls in the most rostral section of tissue only. All abnormalities observed indicate the importance of system x_c^-, in general, and astrocyte system x_c^-, in particular, to construction of proper brain morphology.

Executive Summary

Astrocytes are the most abundant cell type in the central nervous system (CNS) and are essential for creating the structural architecture of the brain by modulating neuronal synapses (Agulhon et al., 2008; Bélanger & Magistretti, 2009; Christopherson et al., 2005). Proper brain functioning depends on chemical factors released by astrocytes that direct neurons to their necessary locations (Clarke & Barres, 2013). Improper migration of cells and, therefore, irregularities in brain structure lead to severe deficits in overall brain function (Moffat, Ka, Jung, & Kim, 2015; Rahimi-Balaei, Bergen, Kong, & Marzban, 2018). Deficits in brain function have also been associated with depleted glutathione (GSH), a thiol antioxidant in the brain largely stored in and released by astrocytes. Continual synthesis of GSH in astrocytes relies on import of cystine, the rate limiting substrate, via the antiporter system x_c^- (O'Connor et al., 1995).

Previous work in the S. Hewett laboratory revealed that system x_c^- is necessary for the formation of normal brain structures. These results were determined using a mouse devoid of system x_c^- in all cell types; however, in the central nervous system, it has been shown that system x_c^- is most abundantly expressed in the astrocytes (Ottestad-Hansen et al., 2018; Pfrieger & Barres, 1997; Pow, 2001). Thus, to determine whether loss of system x_c^- in astrocytes only would alter gross brain morphology, I utilized a transgenic mouse model in which the substrate specific light chain for system x_c^- was deleted [so-called astrocyte conditional null (AcKO) mice].

Brains were harvested from male and female AcKO mice and their wild-type (WT) littermate controls. Gross morphological measurements of hemispheric, hippocampal, striatal, corpus callosal, and lateral ventricular areas, in addition to cortical and corpus callosal widths

were made over the rostro-caudal extent of each brain. Results show a dynamic effect of astrocytic system x_c^- on gross brain morphology in which several brain structures expressed sex-independent atrophy while others showed sex-dependent enlargement. Specifically, the lateral ventricular area was smaller in both male and female AcKO mice when compared to WT littermates. However, the corpus callosum of female AcKO mice was significantly larger than WT controls, an aberration not observed in male mice. The corpus callosum is situated directly above the lateral ventricles, making it possible that these two structures are developmentally linked such that enlargement of the corpus callosum in the female AcKO mice restricted the ventricles from achieving their full size. Additionally, male AcKO mice have a significantly larger striatum than WT controls, a difference not found in female mice. Since the striatum sits adjacent to the lateral ventricle, enlargement of the striatum may have resulted in a similar developmental restriction of ventricular area. Both male and female AcKO mice have larger hippocampal areas than their wild-type controls in the most rostral section of tissue only. Finally, in aggregate the changes observed did not phenocopy those that were found previously using a global null mice, which suggests that changes found in AcKO are either offset by loss of system x_c^- in another cellular subtype in the brain or due to a complex interaction with the genetic background (AcKO are maintained in the C57/Bl6J background, whereas the global null is in C3H/HeSnJ) that could cause the mutation to show distinct phenotypic effects.

Overall, the results from this study suggest that astrocyte system x_c^- plays a significant role in brain morphogenesis occurring in a limited sexual dimorphic manner in C57/Bl6J mice as evident by the structural variation between WT and AcKO mice of both sexes.

Table of Contents

Abstract……ii

Executive Summary……...iii

Acknowledgements……vi

Chapter 1: Introduction……..1

Chapter 2: Methods……4

Generation of Experimental Animals…….……4

Genotyping……4

Tissue Collection……6

Sectioning and Staining……..6

Gross Brain Morphological Analysis……..7

Statistical Analysis……..7

Chapter 3: Results……8

Chapter 4: Discussion……..16

Chapter 5: Future Directions……..19

References……21

Acknowledgements

I would like to express my profound appreciation to my research advisor, Dr. Sandra Hewett, for providing me support, mentorship, and an inspirational example of what it means to be a researcher. I am grateful for the standard that she set and the tools and advice she provided so that I could achieve that standard. I am confident that my research experience has prepared me well for the challenges that lie ahead in my scientific career.

I am extremely grateful for Dr. Sheila M. S. Sears who welcomed me into the lab and passed on the knowledge and skills necessary to complete this project. Her dissertation was the inspiration for this research; my conclusions are built upon the strong foundation she provided.

I would also like to express gratitude to each of my laboratory coworkers, Dr. Carla Frare, Caroline Baggeroer, Kaitlynn Esemaya, Myles Morgan, Heather Sosnoski, Audrey Wood, Nathena Murray, and all of the members of the Dr. James Hewett Laboratory for their assistance and motivation during our years spent together in the lab. Additionally, I would like to thank Audrey Mellan and Andrew Steigerwald for their effort and accuracy when creating measurements of each brain structure.

Finally, I would like to thank my honors reader, Dr. Jessica MacDonald, who provided constructive criticism and helpful suggestions to aid in the completion of this Thesis.

Chapter 1:

Introduction

Astrocytes: Astrocytes are the most numerous cell type in the central nervous system (Jäkel & Dimou, 2017). They are star-shaped glial cells that are necessary for proper development and function of the central nervous system (CNS). Astrocytes are essential in forming the structural architecture of the brain by controlling the dynamic movement of neurons via direct scaffolding and chemoattraction/chemorepulsion (Cayre, Canoll, & Goldman, 2009). Additionally, astrocyte factors promote synapse formation [for review (Chung, Allen, & Eroglu, 2015; Lundgaard, Osório, Kress, Sanggaard, & Nedergaard, 2014)]. They are necessary for the formation and maintenance of the barrier between the brain and blood capillaries, which restricts movements of drugs and toxicants into the brain. Yet, they are important for nutrient entry (Kimelberg, Harold K. & Norenberg, 1989). Substances released by astrocytes control cerebral blood flow, which increases the availability of glucose and oxygen during enhanced neuronal activity (Lundgaard et al., 2014). Astrocytes also recycle neurotransmitters from the extracellular space in order to maintain proper synaptic transmission (Vasile, Dossi, & Rouach, 2017). Finally, astrocytes represent the largest reservoir of the antioxidant γ-glutamylcysteinylglycine, or glutathione (GSH), in the brain (Wang & Cynader, 2002), which they release at a rate of 10% per hour into the extracellular space (Dringen, Kranich, & Hamprecht1, 1997). Continual synthesis is required to maintain optimal levels of GSH in astrocytes for use and extrusion. Cystine is the rate limiting substrate for the production of GSH and is delivered via the transporter system x_c^- (Chowdhury, Allen, Thorn, He, & Hewett, 2018; He, Jackman, Thorn, Vought, & Hewett, 2015).

System x_c^-: System x_c^- is a heterodimeric amino acid transporter that imports extracellular cystine and exports intracellular glutamate in a one to one fashion [for review see (Lewerenz et al., 2013)]. System x_c^- is comprised of a heavy chain, 4f2hc, and a substrate specific light chain, xCT, covalently linked with a disulfide bond (Zhang et al., 2014). In the CNS, system x_c^- is detected in most brain areas with especially high abundance in astrocytes (Fournier et al., 2017; Ottestad-Hansen et al., 2018; Pow, 2001; Zhang et al., 2014). To study the role of system x_c^- in biological systems, null mutant mice are often employed. Scientist have created and studied a genetically modified mouse, which was engineered to remove xCT ($xCT^{-/-}$) (Sato et al., 2005). Others, including our lab, study the C3H/HeJ (C3H) *SLC7a11*$^{sut/sut}$ mouse, which harbors a natural null mutation in *SLC7a11*, the gene that encodes for xCT. Both of these mice models are considered global nulls, meaning that all cells are devoid of system x_c^-.

Brain atrophy and sexual dimorphism: Nearly 15 year ago, Tim Murphy and colleagues reported that *SLC7a11*$^{sut/sut}$ male mice, at 14 weeks of age, demonstrate brain atrophy (Shih et al., 2006), suggesting system x_c^- was important for maintaining neuronal survival. Female mice were not included in this study. Since brain morphological differences between sexes (i.e. sexual dimorphism) exists (Allen, Damasio, Grabowski, Bruss, & Zhang, 2003; Chen, Sachdev, Wen, & Anstey, 2007; Im et al., 2006; Nopoulos, Flaum, O'leary, & Andreasen, 2000), a previous graduate student in the S. Hewett lab, repeated this study using both male and female C3H-*SLC7a11*$^{sut/sut}$ mice and compared gross brain morphology to their sex- and age-matched C3H-*SLC7a11*$^{+/+}$ littermate controls to determine whether female mice would suffer the same fate. In contrast to the study of Shih and colleagues, our laboratory found no gross brain atrophy in either

males or females. Despite this, sexual dimorphic changes between C3H-*SLC7a11*$^{sut/sut}$ and C3H-*SLC7a11*$^{+/+}$ mice at the gross and cellular level were identified.

Specifically, female C3H-*SLC7a11*$^{sut/sut}$ mice have smaller cell bodies, or soma, than female C3H-*SLC7a11*$^{+/+}$ littermates, a morphological alternation not observed in males (Sears, 2018). Conversely, male C3H-*SLC7a11*$^{sut/sut}$ mice show increased dendritic complexity as compared to their C3H-*SLC7a11*$^{+/+}$ littermate male controls. This change in complexity is not seen in females (Sears, 2018). Finally, female C3H-*SLC7a11*$^{sut/sut}$ mice have a statistically significant smaller corpus callosum than female C3H-*SLC7a11*$^{+/+}$ mice (Sears, 2018). This same morphological aberration is not observed in male counterparts. Finally, there were no morphological differences found in cortical width or ventricular, striatal, hippocampal, and total hemispheric areas between genotypes in either males or females.

As mentioned above, C3H-*SLC7a11*$^{sut/sut}$ mice are globally null for system x_c^-; yet in the CNS, system x_c^- is found predominately in the astrocyte cell population. Thus, the overall goal of my thesis was to determine whether the elimination of system x_c^- in the astrocyte cell population *only* would phenocopy the changes in gross morphology determined previously in the C3H-*SLC7a11*$^{sut/sut}$ male and female mice. Toward this end, I utilized C57/Bl6J (B6) astrocyte conditional system x_c^- knockout mice (B6-mGFAP-Cre-SLC7a11$^{fl/fl}$ or AcKO mice).

Overall Hypothesis: Sexual dimorphic brain morphological differences in AcKO mouse will recapitulate those determined in the C3H-*SLC7a11*$^{sut/sut}$ mouse.

Chapter 2:

Methods

All mice were used in accordance with the National Institutes of Health guidelines for the use of experimental animals as approved by the Institutional Animal Care and Use Committee of Syracuse University. Mice were housed in the Laboratory Animal Resource facility at Syracuse University on a 12-hour light/ dark schedule and provided food and water *ad libitum*.

Generation of Experimental Animals: Female hemizygous C57/Bl6J (B6) mGFAP-Cre mice (The Jackson Laboratory 024098) were bred with males who have exon 2 of *SLC7a11* gene flanked by LoxP sites (B6-*SLC7a11*$^{fl/fl}$). The resulting male B6-*SLC7a11*$^{+/fl}$ were bred with female B6-mGFAP-Cre-*SLC7a11*$^{+/fl}$. This breeding paradigm created wild type (B6-*SLC7a11*$^{+/+}$, B6-mGFAP-Cre-*SLC7a11*$^{+/+}$, and B6-*SLC7a11*$^{fl/fl}$) and AcKO (B6-mGFAP-Cre-*SLC7a11*$^{fl/fl}$) mice. At weaning, pups were separated by sex and marked for identification using ear-punch. Genotyping was performed via PCR analysis of tail genomic DNA samples.

Genotyping: Upon weaning, approximately 0.5 cm of tail was removed and dissolved in 500 µL of lysis buffer (100 mM Tris, pH 7.4, 500mM NaCl, 0.2% SDS, 5mM EDTA, and 100 µg/mL proteinase K) at 55°C for no more than 72 hours. Samples were spun for 5 minutes at 10,000xg at room temperature to remove cellular debris, after which supernatant was decanted into a new tube containing molecular grade isopropanol. Following manual inversion after which DNA was visible, samples were re-spun, supernatant was removed and ice-cold 70% EtOH added to the precipitant DNA. EtOH was removed and the DNA suspended in 200-500 µL

DNAse-free H_2O. DNA concentrations were determined using a NanoDrop microvolume spectrophotometer.

The presence of Cre in the genome was determined by touchdown PCR. Three μL of DNA was combined with a master mixture containing 1.3x of PCR buffer (Invitrogen, Carlsbad, CA), 2.6 mM $MgCl_2$, 0.26 mM dNTP, 6.5% glycerol (Sigma Chemical Co., St. Louis, MO), 0.03 U/μL *Taq* polymerase (Invitrogen, Carlsbad, CA), and 0.5 μM of the following primers for a final volume of 15 μL.

Cre primers:

Cre P1:	5' – TCC ATA AAG GCC CTG ACA TC – 3'
Cre P2:	5' – TGC GAA CCT CAT CAC TCG T – 3'
Cre Internal Control 1:	5' – CAA ATG TTG CTT GTC TGG TG – 3'
Cre Internal Control 2:	5' – GTC AGT CGA GTG CAC AGT TT – 3'

Cre P1 and P2, which is indicative of mGFAP-Cre allele produced an amplicon of 400 bp. Cre Internal Control 1 and 2, which produces an amplicon of 200 bp, serves as a positive control for the reaction. Reactions containing Cre P1, P2 and Cre Internal Control 1 and 2 were "touched down" from 94°C to 63°C over the course of 10 cycles to promote desired product amplification. The samples were melted at 94°C for 15 sec, annealed at 60°C for 15 sec, and elongated at 72°C for 10 sec over the course of 28 cycles using a Thermal Cycler (Bio-Rad, C1000 Touch).

To determine wild-type (WT) or floxed alleles, 3 μL of DNA was combined with a master mixture containing 1x of PCR buffer (Invitrogen, Carlsbad, CA), 1.5 mM $MgCl_2$, 0.2 mM dNTP, 10% DMSO, 0.02 U/μL *Taq* polymerase (Invitrogen, Carlsbad, CA), and 0.5 μL of the following primers for a final volume of 15 μL.

Primers:

Forward: 5’ – AAC AGC TCT AGG CAG ACG TG – 3’

Reverse: 5’ – TCA GCT ACC CTG CCT CAA AC – 3’

were used to amplify 1100 bp (indicative of a WT allele) and/or 1255 bp (indicative of a floxed allele) fragments of DNA. Reactions were melted at 94°C for 225 sec, annealed at 60°C for 30 sec, and elongated at 72°C for 100 sec for 34 cycles.

Tissue Collection: Brain tissue was collected from 6 female and 6 male B6-*SLCa11*$^{+/+}$ mice, 6 female and 6 male B6-mGFAPCre-*SLC7a11*$^{+/+}$ mice, and 6 female and 6 male B6-mGFAPCre-*SLC7a11*$^{fl/fl}$ mice between 14-23 weeks of age. Deeply anesthetized mice (1 mL isoflurane anesthesia) were euthanized via cervical dislocation, followed by decapitation. The cranial vault was accessed by removal of the calvaria, the brain was removed, and immediately embedded in a cryomold of Optimal Cutting Temperature (O.C.T.) compound (Tissue Tek, Torrance, CA). The cryomold was frozen in a bath of dry ice containing 140-proof ethyl alcohol and stored in the -80°C freezer until sectioning.

Sectioning and Staining: Frozen brain sections (coronal, 40 µm) were collected serially between +1.1 mm and -2.54 mm relative to bregma using a cryostat (Thermo Fisher Scientific, Microm HM550). Slices were mounted on SuperFrost Plus slides (Fisher Scientific, Houston, TX). The sections were dyed using a cell-specific 0.5% thionin stain as described in detail (Chowdhury et al., 2018). Briefly, the slides were submerged in a series of solutions (70% EtOH, ddH_2O, thionin, ddH_2O, ddH_2O, 70% EtOH, 95% EtOH, 100% EtOH, 100% Xylene, 100%

Xylene). Following staining, a cover slip was applied and the slides were stored in a light-sensitive box at room temperature.

Gross Brain Morphological Analysis: Gross brain morphological measurements were made on scanned images (Epson 3170; 720 dpi) using the NIH computer software Image J (version 1.47v) over the rostro-caudal extent of each brain (+1.1, -0.1, -0.94, -1.46, -2.54 relative to bregma) by three measurers blind to the mouse's genotype. Using the freehand selection tool, three measurements of each area (lateral ventricle, striatum, corpus callosum, and hippocampus) were made on the left and the right by each measurer for a total of six measurements per structure (three measurements total for structures crossing the midline). Data are expressed as the mean ventricular, striatal, hemispheric, and hippocampal areas determined by averaging the mean calculated from all three individuals. Mean corpus callosum width was obtained by averaging three non-overlapping measurements using the straight line tool from the apex to the base of the corpus callosum at the midline. Mean cortical width was obtained by averaging six non-overlapping (3 bilateral) measurements using the straight tool from the apex of the corpus callosum to the pial layer in between the somatosensory and motor cortices. All data are expressed as the average measurements obtained for each area in each mouse for each genotype derived from the mean calculated from all three individuals.

Statistical Analysis: Statistical significance between genotypes was determined by two-way ANOVA at significance level 0.05 followed by a Bonferroni correction for multiple comparisons. All statistical analyses were performed using GraphPad Prism (Version 8.03, GraphPad Software Inc.).

Chapter 3:

Results

Statistics: Statistical significance between genotypes was determined by two-way ANOVA followed by a Bonferroni correction for multiple comparisons. The probability value (p-value) determines the probability at which a given outcome will occur by chance. Asterisks represent values that are significantly different at the same distance from bregma. P-values less than 0.05 are indicated by one asterisk (*), less than 0.01 are designated by two (**), less than 0.001 are shown by three (***), and less than 0.0001 are specified by four asterisks (****).

Gross Morphological Assessment of Female brains: Measurements of several gross brain structures were made over the rostral-caudal extent of each brain sections (+1.1mm to -2.54mm from bregma) from B6-mGFAP-Cre-*SLC7a11*$^{+/+}$ (B6-WT+Cre) and B6-mGFAP-Cre-*SLC7a11*$^{fl/fl}$ (AcKO) mice and compared (Figure 1). Neither hemispheric area (Figure 1B) nor striatal area (Figure 1E) show any between group (i.e., genotype) differences. While the overall cortical width is not different between the genotypes ($p = 0.6988$), there is a significant increase in AcKO female mice cortical width at bregma distance +1.1 ($p < 0.01$; Figure 1C). No genotype difference in hippocampal area is noted ($p = 0.0577$), although at section -1.46mm, the area of AcKO animal is greater than B6-WT+Cre control mice ($p < 0.05$; Figure 1D). Corpus callosal area of AcKO mice is significantly larger than B6-WT+Cre at -0.1mm ($p < 0.01$) and -0.94mm ($p < 0.001$) from bregma, which contributes to an overall genotype difference ($p = 0.0011$; Figure 1F). There is no significant between group differences in corpus callosum width (Figure 1G). Finally, the overall lateral ventricular area is significantly smaller in AcKO mice as compared to their B6-WT+Cre controls (genotype difference: $p = 0.0011$, Figure 1H). This change is driven by reductions at bregma distances +1.1 ($p < 0.05$) and -0.94 ($p < 0.01$; Figure 1H).

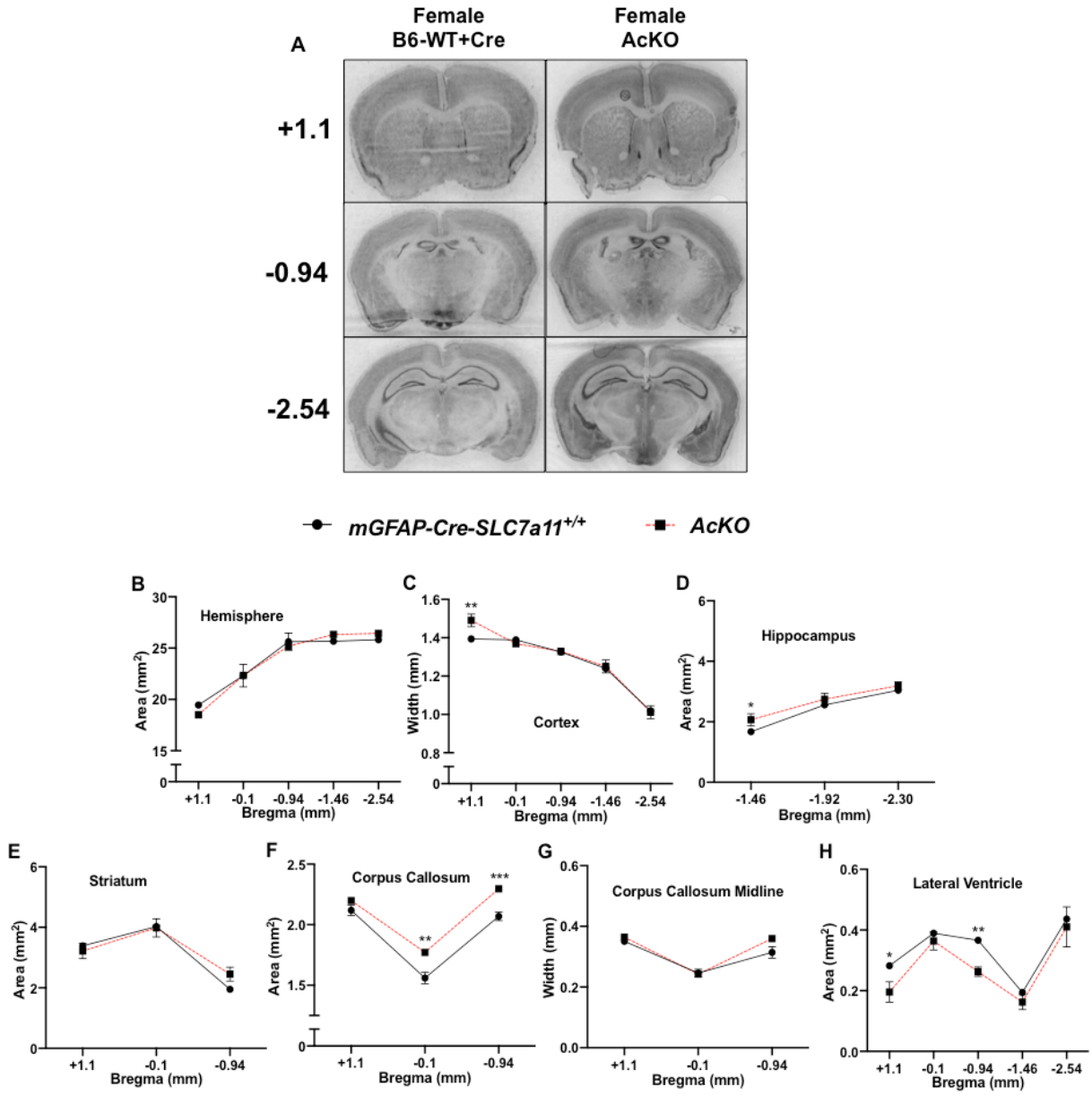

Figure 1. Comparison of female B6-mGFAP-Cre-*SLC7a11*$^{+/+}$ and AcKO gross brain morphology.

(A) Representative thionin stained slices (rostral-caudal- +1.1mm, -0.94mm, and -2.54mm from bregma) of female B6-mGFAP-Cre-*SLC7a11*$^{+/+}$ [B6-WT+Cre (left)] and B6-mGFAP-Cre-*SLC7a11*$^{fl/fl}$ [AcKO (right)] mice. **(B-H)** Area or width measurements for each respective brain structure. B6-WT+Cre animals are represented by the solid black line, whereas the AcKO animals are represented by the dashed red line. Measurements taken from B6-WT+Cre were used for both Figure 1 and Figure 2. n=6 mice in each group spanning 14-23 weeks of age. * $p < 0.05$; ** $p < 0.01$; ***$p < 0.001$ as determined two-way ANOVA followed by a Bonferroni correction for multiple comparisons.

Because these results differed from those found in the global C3H-*SLC7a11*$^{sut/sut}$ mice (Sears, 2018), where the tendency is for brain areas/widths to be smaller than their wild-type littermate controls (C3H-*SLC7a11*$^{+/+}$), I next assessed whether the presence of Cre-recombinase impacted gross brain morphology on its own. Thus, identical measurements to those described above were made in littermate female B6-*SLC7a11*$^{+/+}$ (B6-WT), which lack Cre-recombinase, and compared to the same B6-WT+Cre mice already analyzed and reported for Figure 1 (Figure 2). While there is no overall genotype difference in hemispheric area ($p = 0.9189$), B6-WT+Cre, exhibit a larger hemispheric area at bregma distance -0.1 as compared to B6-WT mice not containing Cre-recombinase ($p < 0.0001$; Figure 2B). However, the hemispheric area at -0.94mm from bregma of B6-WT+Cre is smaller ($p < 0.05$; Figure 2B). Cortical widths do not differ between genotypes ($p = 0.7885$) or at any distance from bregma (Figure 2C). Hippocampal area does not show a significant genotype difference ($p = 0.0839$), although at the level of -2.30 mm from bregma, the area of the female B6-WT+Cre animal is larger than that of the B6-WT mice ($p < 0.05$; Figure 2D). With respect to the striatal area, there is no difference between genotypes, in general ($p = 0.7087$), or at any distance from bregma (Figure 2E). Interestingly, female B6-WT+Cre mice exhibit a significantly larger corpus callosal area than female B6-WT mice at -0.94mm from bregma ($p < 0.05$), but do not show an overall genotype effect ($p = 0.9552$; Figure 2F). No significant differences are seen between B6-WT and B6-WT+Cre regarding corpus callosum width (Figure 2G). Overall, a significant decrease in the lateral ventricular area is found in female B6-WT+Cre mice as compared to B6-WT mice (overall genotype difference: $p = 0.0143$), despite no significant differences at any specific distance from bregma (Figure 2H). Female wild-type mice with and without Cre-recombinase show various structural differences that suggest that the presence of Cre-recombinase does impact gross brain morphology.

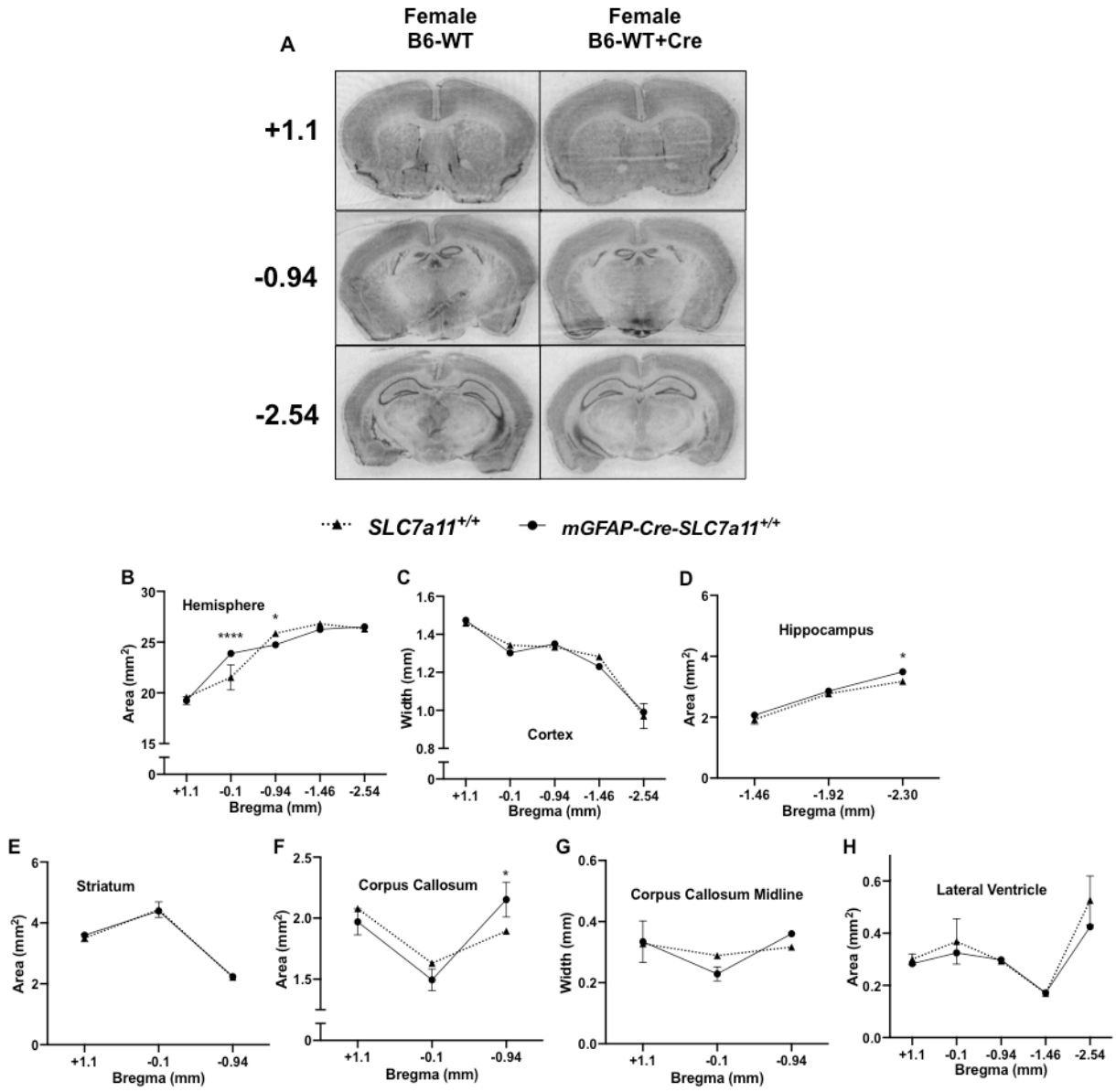

Figure 2. Comparison of female B6-mGFAP-Cre-*SLC7a11*$^{+/+}$ and B6-*SLC7a11*$^{+/+}$ gross brain morphology.

(A) Representative thionin stained slices (rostral-caudal- +1.1mm, -0.94mm, and -2.54mm from bregma) of female B6-*SLC7a11*$^{+/+}$ [B6-WT (left)] and B6-mGFAP-Cre-*SLC7a11*$^{+/+}$ [B6-WT+Cre (right)] mice. **(B-H)** Area or width measurements for each respective brain structure. B6-WT animals are represented by the dashed line, whereas B6-WT+Cre animals are represented by the solid line. Measurements taken from B6-WT+Cre were used for both Figure 1 and Figure 2. n=6 mice in each group spanning 14-23 weeks of age. * $p < 0.05$; ** $p < 0.01$; ***$p < 0.001$; **** $p < 0.0001$ as determined two-way ANOVA followed by a Bonferroni correction for multiple comparisons.

Gross Morphological Assessment of Male brains: To assess the potential sex-dependence of the changes described above, measurements identical to those previously stated in females were made in male B6-WT+Cre and AcKO mice (Figure 3). The cerebral hemisphere area is significantly larger in AcKO animals at nearly all levels of bregma [-0.94 ($p < 0.0001$), -1.46 ($p < 0.0001$), and -2.54 ($p < 0.001$)] resulting in an overall genotype difference in males ($p < 0.0001$) (Figure 3B). There is no overall genotype difference ($p = 0.9711$) or a significant difference at any distance from bregma in cortical width (Figure 3C). While overall hippocampal area is similar between genotypes ($p = 0.8111$), AcKO animals show a significant increase in hippocampal area at level -1.46mm from bregma ($p < 0.05$; Figure 3D). The striatal area is significantly different between genotypes ($p = 0.0014$), driven almost solely by increases at bregma distance -0.94 ($p < 0.01$) in the male AcKO (Figure 3E). Neither corpus callosal area (Figure 3F), nor width (Figure 3G) show a difference between genotypes or at any distance from bregma. There is an overall genotype difference ($p = 0.0265$) in lateral ventricular area between male AcKO and B6-WT+Cre mice as a result of reduced ventricular area in AcKO mice determined at -2.54mm from bregma ($p < 0.001$; Figure 3H).

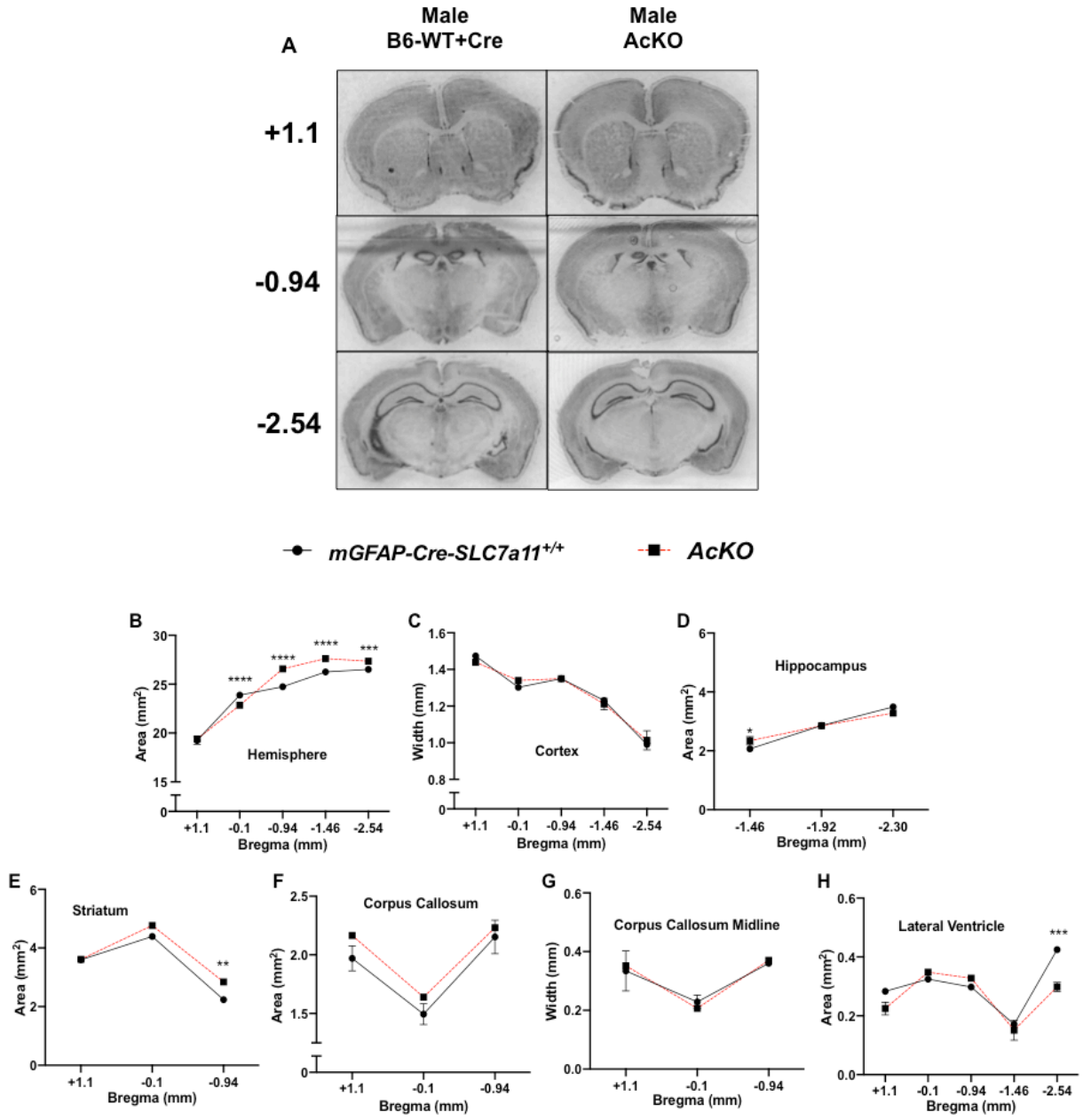

Figure 3. Comparison of male B6-mGFAP-Cre-*SLC7a11*$^{+/+}$ and AcKO gross brain morphology.

(A) Representative thionin stained slices (rostral-caudal- 1.1mm, -0.94mm, and -2.54mm from bregma) of male B6-mGFAP-Cre-*SLC7a11*$^{+/+}$ [B6-WT+Cre (left)] and B6-mGFAP-Cre-*SLC7a11*$^{fl/fl}$ [AcKO (right)] mice. **(B-H)** Area or width measurements for each respective brain structure. B6-WT+Cre animals are represented by the solid black line, whereas AcKO animals are represented by the dashed red line. Measurements taken from B6-WT+Cre were used for both Figure 3 and Figure 4. n=6 mice in each group spanning 14-23 weeks of age. * $p < 0.05$; ** $p < 0.01$; ***$p < 0.001$; **** $p < 0.0001$ as determined two-way ANOVA followed by a Bonferroni correction for multiple comparisons.

To determine if Cre-recombinase had an effect on male brain morphology independent of changes in system x_c^-, identical measurements were made in (B6-WT) and compared to the B6-WT+Cre mice already analyzed and reported for Figure 3 (Figure 4). Hemisphere area of male B6-WT and B6-WT+Cre mice show no between-group difference ($p = 0.8087$; Figure 4B), although a significant increase in area was noted in B6-WT+Cre mice at -0.1mm from bregma ($p < 0.001$), which is off-set by a decrease at -1.46mm from bregma ($p < 0.01$) when compared to B6-WT animals (Figure 4B). There is no between group difference in cortical width ($p = 0.3773$) or at any level of bregma ($p > 0.05$; Figure 4C). Likewise, there is no overall difference in hippocampal area between genotypes ($p = 0.2246$), or at any distance from bregma ($p > 0.05$; Figure 4D). Additionally, the striatal area shows no overall genotype difference ($p = 0.5891$), nor is there any significant difference at any distance from bregma ($p > 0.05$; Figure 4E). Neither corpus callosal area ($p = 0.4348$; Figure 4F), nor width ($p = 0.4385$; Figure 4G) differ between genotypes. Finally, there is no difference in lateral ventricular area between genotypes, in general ($p = 0.9745$) or at any distance from bregma ($p > 0.05$; Figure 4H). Overall, the presence of Cre-recombinase in male wild-type mice only impacted hemisphere area. These data suggest that Cre-recombinase does not have as great of an impact on male brain morphology as it does on female brain morphology.

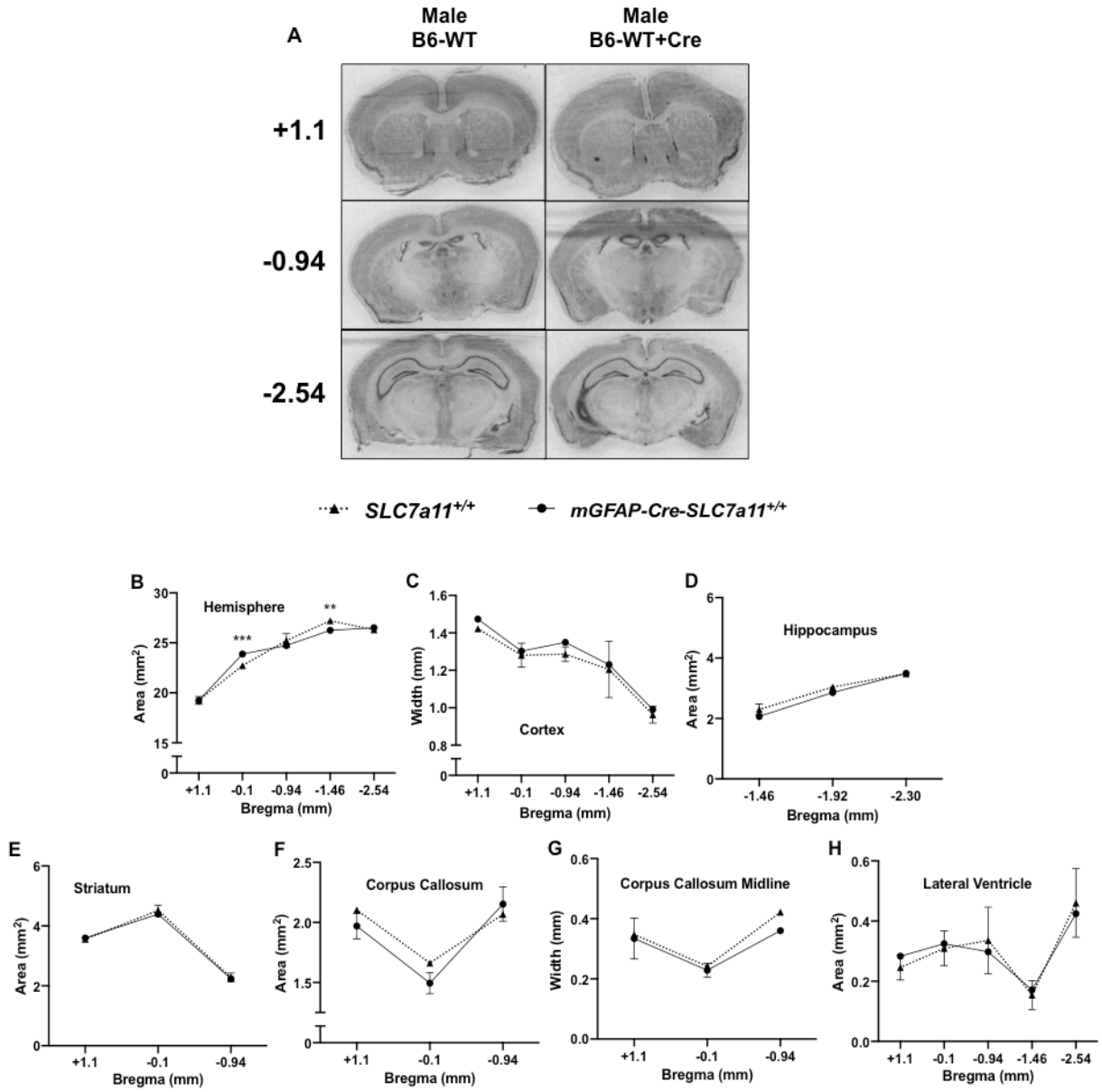

Figure 4. Comparison of male B6-mGFAP-Cre-*SLC7a11*$^{+/+}$ and B6-*SLC7a11*$^{+/+}$ gross brain morphology.

(A) Representative thionin stained slices (rostral-caudal- +1.1mm, -0.94mm, and -2.54mm from bregma) of male B6-*SLC7a11*$^{+/+}$ [B6-WT (left)] and B6-mGFAP-Cre-*SLC7a11*$^{+/+}$ [B6-WT+Cre (right)] mice. **(B-H)** Area or width measurements for each respective brain structure. B6-WT animals are represented by the dashed line, whereas B6-WT+Cre animals are represented by the solid line. Measurements taken from B6-WT+Cre were used for both Figure 3 and Figure 4. n=6 mice in each group spanning 14-23 weeks of age. * $p < 0.05$; ** $p < 0.01$; ***$p < 0.001$ as determined two-way ANOVA followed by a Bonferroni correction for multiple comparisons.

Chapter 4:

Discussion

Results from the present study suggest that astrocyte system x_c^- plays a significant role in brain morphogenesis — as evident by the structural variation between WT and AcKO mice — and that this occurs in a limited sexual dimorphic manner. Additionally, results suggest that Cre-recombinase has an effect on some aspects of brain morphology, since several structures in B6-WT+cre mice also exhibit abnormalities in a sexually dimorphic manner, with greater effect on the female mouse brain. However, the aberrations observed in wild-type animals with Cre-recombinase are not significant enough to account for the morphological differences observed in AcKO mice that also contain Cre-recombinase. Therefore, the loss of astrocyte system x_c^- is responsible for the aberrations observed in AcKO mice since it exerts a greater effect on brain morphology than the presence of Cre-recombinase alone.

Specifically, we found that lateral ventricular area in both AcKO males and females is significantly decreased as compared to B6-WT+Cre littermates. Lateral ventricles are cavities in the brain that contain cerebrospinal fluid (CSF). CSF plays an important role in the protection and homeostasis of neural tissue (Filis, Aghayev, & Vrionis, 2017) in addition to the circulation of nutrients and removal of waste (Proescholdt, Hutto, Brady, & Herkenham, 2000). Ventricular abnormalities are found in diverse neurological conditions including schizophrenia (Sowell et al., 2000), Alzheimer's disease (Nestor et al., 2008), and epilepsy (Jackson et al., 2011). Of interest, this decrease was not observed in the global null (C3H-*SLC7a11*$^{sut/sut}$) animal (Sears, 2018), which suggests that changes found in AcKO are offset by loss of system x_c^- in another cellular subtype in brain. Alternatively, this could be due to a complex interaction with the genetic background that could cause the mutation to show distinct phenotypic effects, since our AcKO

are maintained in the C57/Bl6J background, whereas the global null is in C3H/HeSnJ. Our experimental design does not allow me to distinguish whether this decrease in ventricular size results from cellular loss, i.e. atrophy, or a primary defect in ventricular development. However, it is intriguing to speculate that ventricular reduction in AcKO mice might be linked to the enlargement of corpus callosum and striatum in females and male mice, respectively.

The corpus callosum is a white matter fiber tract that sits beneath the cerebral cortex and maintains interhemispheric connections by coordinating activity between contralateral areas (Asadi-Pooya, Sharan, Nei, & Sperling, 2008). Variations in area of this structure are comorbid with several disorders including autism, Alzheimer's, and epilepsy (Im et al., 2006; Mainen & Sejnowski, 1996; Scharfman, 2007). Whether this change is associated with any behavioral alterations was not addressed by my studies. As was the case for ventricles, current observations do not recapitulate that of the previous doctoral student's in which the corpus callosum was found to be smaller in female C3H-*SLC7a11*$^{sut/sut}$ mice, demonstrating again that loss of system x_c^- function in astrocytes only does not phenocopy the global null as was originally hypothesized.

The basal ganglia is located deep within the cerebral hemispheres and functions in both motor and reward systems. The largest subcortical nucleus of the basal ganglia is the striatum, which is comprised of the caudate nucleus, the putamen, and the globus pallidus (Lanciego, Luquin, & Obeso, 2012). The striatum relies heavily on input from the neurotransmitter dopamine to transmit signals to the rest of the basal ganglia (Lanciego et al., 2012). These dopaminergic inputs stimulate motor planning, reinforcement, reward perception, and play a large role in addiction (Yager, Garcia, Wunsch, & Ferguson, 2015). If the enlargement found in male AcKo is associated with an increase in dopaminergic innervation, which has not yet been determined, then these mice could have heightened striatum-dependent cued learning, and show

better performance on navigational memory tasks when environmental cues are present (Baldan Ramsey & Pittenger, 2010; Ferbinteanu, 2016). The striatal memory system functions independently and in parallel with the hippocampal memory system, which processes spatial information (Lee, Duman, & Pittenger, 2008). Both male and female AcKO mice exhibit a larger hippocampal area than their B6-WT+Cre littermates.

The hippocampus is comprised of densely packed neurons and is a component of the limbic system, responsible for emotional perception and regulation (Anand & Dhikav, 2012). The hippocampus is situated deep within the medial temporal lobe and plays a significant role in learning and memory processes, specifically spatial learning. Thus, it is intriguing to speculate that female AcKO mice, who show no change in striatal area, will rely more on hippocampal memory systems and thus perform with greater success on spatial learning, rather than cue-based, tasks, than sex-matched B6-WT+Cre littermate controls. Since male AcKO mice show enlargement of both striatum and hippocampus, it is possible that they will demonstrate an overall enhancement of memory as compared to sex- and age-matched B6-WT+Cre control mice. It is also possible that these two memory systems compete with one another during learning (Poldrack et al., 2001).

Overall, we find that the gross morphological changes found in AcKO of both sexes do not phenocopy to those determined in global null C3H-*SLC7a11*$^{sut/sut}$ mouse. This failure to recapitulate prior findings using astrocyte conditional null animals suggests that the observations made in the C3H-*SLC7a11*$^{sut/sut}$ mice could be a result from something other than simple loss of function of system x_c^- in astrocytes, or these discrepant findings could result from background effects. Despite this, sexually dimorphic morphological differences observed in this study indicate the importance of astrocyte system x_c^- in brain morphogenesis of both sexes.

Chapter 5:

Future Directions

With direct relevance to this study, further studies should be conducted to determine the impact of Cre-recombinase on gross brain morphogenesis. This study unexpectedly found significant effects on brain morphology due to the presence of Cre-recombinase in B6-WT+Cre animals. In the breeding paradigm, a mouse that is devoid of astrocyte system x_c^- but does not contain Cre-recombinase (B6-*SLC7a11*$^{fl/fl}$) is produced. Therefore, a further study to make morphological comparisons between B6-mGFAP-Cre-*SLC7a11*$^{fl/fl}$ (AcKO) and B6-*SLC7a11*$^{fl/fl}$ mice will be necessary in order to fully determine the impact that Cre-recombinase has on brain morphology.

The mechanism responsible for morphological differences observed in the experimental mice cannot be determined with confidence. The changes could be a result of cellular gain/loss or developmental in nature. In order to determine the driving force of morphological aberrations, it would be necessary to harvest tissue and analyze structures at several points during development, rather than waiting until the brain is fully formed.

Smaller soma size was a sex-dependent change previously observed in female C3H-*SLC7a11*$^{sut/sut}$ mice. Another sexual dimorphic difference is observed in male C3H-*SLC7a11*$^{sut/sut}$ mice, which show increased dendritic complexity compared to their C3H-*SLC7a11*$^{+/+}$ littermate controls. This study should be repeated using the astrocyte conditional null animals to determine if the loss of system x_c^- in astrocytes would phenocopy the neuronal phenotypes identified in global null animals.

The loss of system x_c^- has the potential to alter both glutamate and GSH levels. A future study could compare levels of glutamate and GSH between C3H-*SLC7a11*$^{sut/sut}$ and B6-AcKO mice of both sexes to determine if the changes in morphology observed occurs in association with alterations in either or both of these molecules.

Since the observations made in this experiment did not phenocopy those previously made in the global null animals, we cannot conclude with certainty that astrocyte system x_c^- was responsible for the initially observed sex-dependent differences in C3H-*SLC7a11*$^{sut/sut}$ mice. A future experiment should use a promoter to drive Cre-recombinase, which will remove *SLC7a11* from all cells in order to mirror the global null C3H-*SLC7a11*$^{sut/sut}$ mouse. Should this not recapitulate what is found in the C3H-*SLC7a11*$^{sut/sut}$ mice, we would have to conclude that strain-dependent differences underlie the phenotype.

References:

Agulhon, C., Petravicz, J., McMullen, A. B., Sweger, E. J., Minton, S. K., Taves, S. R., … McCarthy, K. D. (2008, September 25). What Is the Role of Astrocyte Calcium in Neurophysiology? *Neuron*, Vol. 59, pp. 932–946. https://doi.org/10.1016/j.neuron.2008.09.004

Allen, J. S., Damasio, H., Grabowski, T. J., Bruss, J., & Zhang, W. (2003). Sexual dimorphism and asymmetries in the gray-white composition of the human cerebrum. *NeuroImage*, *18*(4), 880–894. https://doi.org/10.1016/S1053-8119(03)00034-X

Anand, K., & Dhikav, V. (2012, October). Hippocampus in health and disease: An overview. *Annals of Indian Academy of Neurology*, Vol. 15, pp. 239–246. https://doi.org/10.4103/0972-2327.104323

Asadi-Pooya, A. A., Sharan, A., Nei, M., & Sperling, M. R. (2008). *Corpus Callosotomy*. https://doi.org/10.1016/j.yebeh.2008.04.020

Baldan Ramsey, L. C., & Pittenger, C. (2010). Cued and spatial learning in the water maze: Equivalent learning in male and female mice. *Neuroscience Letters*, *483*(2), 148–151. https://doi.org/10.1016/j.neulet.2010.07.082

Bélanger, M., & Magistretti, P. J. (2009). The role of astroglia in neuroprotection. *Dialogues in Clinical Neuroscience*, Vol. 11, pp. 281–296. Les Laboratoires Servier.

Cayre, M., Canoll, P., & Goldman, J. E. (2009). Cell migration in the normal and pathological postnatal mammalian brain. *Progress in Neurobiology*, *88*(1), 41–63. https://doi.org/10.1016/j.pneurobio.2009.02.001

Chen, X., Sachdev, P. S., Wen, W., & Anstey, K. J. (2007). Sex differences in regional gray matter in healthy individuals aged 44-48 years: A voxel-based morphometric study. *NeuroImage*, *36*(3), 691–699. https://doi.org/10.1016/j.neuroimage.2007.03.063

Chowdhury, T., Allen, M. F., Thorn, T. L., He, Y., & Hewett, S. J. (2018). Interleukin-1β protects neurons against oxidant-induced injury via the promotion of astrocyte glutathione production. *Antioxidants*, *7*(8). https://doi.org/10.3390/antiox7080100

Christopherson, K. S., Ullian, E. M., Stokes, C. C. A., Mullowney, C. E., Hell, J. W., Agah, A., … Barres, B. A. (2005). Thrombospondins Are Astrocyte-Secreted Proteins that Promote CNS Synaptogenesis. *Cell*, *120*, 421–433. https://doi.org/10.1016/j.cell.2004.12.020

Chung, W. S., Allen, N. J., & Eroglu, C. (2015). Astrocytes control synapse formation, function, and elimination. *Cold Spring Harbor Perspectives in Biology*, *7*(9). https://doi.org/10.1101/cshperspect.a020370

Clarke, L. E., & Barres, B. A. (2013). The function of astrocytes in neural circuits. *Nature*, *14*, 311–321. https://doi.org/10.1038/nrn3484

Dringen, R., Kranich, O., & Hamprecht1, B. (1997). The 7-Glutamyl Transpeptidase Inhibitor Acivicin Preserves Glutathione Released by Astroglial Cells in Culture. In *Neurochemical Research* (Vol. 22).

Ferbinteanu, J. (2016). Contributions of hippocampus and striatum to memory-guided behavior depend on past experience. *Journal of Neuroscience*, *36*(24), 6459–6470. https://doi.org/10.1523/JNEUROSCI.0840-16.2016

Filis, A. K., Aghayev, K., & Vrionis, F. D. (2017). *The physiology of CSF is a complex topic, and treatment for hydrocephalus typically depends on its cause. Cerebrospinal Fluid and Hydrocephalus: Physiology, Diagnosis, and Treatment* (Vol. 24).

Fournier, M., Monin, A., Ferrari, C., Baumann, P. S., Conus, P., & Do, K. (2017). Implication of the glutamate-cystine antiporter xCT in schizophrenia cases linked to impaired GSH synthesis. *Npj Schizophrenia*, *3*(1). https://doi.org/10.1038/s41537-017-0035-3

He, Y., Jackman, N. A., Thorn, T. L., Vought, V. E., & Hewett, S. J. (2015). Interleukin-1β protects astrocytes against oxidant-induced injury via an NFκB-dependent upregulation of glutathione synthesis. *Glia*, *63*(9), 1568–1580. https://doi.org/10.1002/glia.22828

Im, K., Lee, J. M., Lee, J., Shin, Y. W., Kim, I. Y., Kwon, J. S., & Kim, S. I. (2006). Gender difference analysis of cortical thickness in healthy young adults with surface-based methods. *NeuroImage*, *31*(1), 31–38. https://doi.org/10.1016/j.neuroimage.2005.11.042

Jackson, D. C., Irwin, W., Dabbs, K., Lin, J. J., Jones, J. E., Hsu, D. A., … Hermann, B. P. (2011). Ventricular enlargement in new-onset pediatric epilepsies. *Epilepsia*, *52*(12), 2225–2232. https://doi.org/10.1111/j.1528-1167.2011.03323.x

Jäkel, S., & Dimou, L. (2017, February 13). Glial cells and their function in the adult brain: A journey through the history of their ablation. *Frontiers in Cellular Neuroscience*, Vol. 11. https://doi.org/10.3389/fncel.2017.00024

Kimelberg, Harold K. & Norenberg, M. D. (1989). Astrocytes. *Scientific American*, *260*(4), 66–77.

Lanciego, J. L., Luquin, N., & Obeso, J. A. (2012). Functional neuroanatomy of the basal ganglia. *Cold Spring Harbor Perspectives in Medicine*, *2*(12). https://doi.org/10.1101/cshperspect.a009621

Lee, A. S., Duman, R. S., & Pittenger, C. (2008). A double dissociation revealing bidirectional competition between striatum and hippocampus during learning. In *PNAS November* (Vol. 4).

Lewerenz, J., Hewett, S. J., Huang, Y., Lambros, M., Gout, P. W., Kalivas, P. W., … Maher, P. (2013, February 10). The cystine/glutamate antiporter system xc- in health and disease: From molecular mechanisms to novel therapeutic opportunities. *Antioxidants and Redox Signaling*, Vol. 18, pp. 522–555. https://doi.org/10.1089/ars.2011.4391

Lundgaard, I., Osório, M. J., Kress, B. T., Sanggaard, S., & Nedergaard, M. (2014, September

12). White matter astrocytes in health and disease. *Neuroscience*, Vol. 276, pp. 161–173. https://doi.org/10.1016/j.neuroscience.2013.10.050

Mainen, Z. F., & Sejnowski, T. J. (1996). Influence of dendritic structure on firing pattern in model neocortical neurons. *Nature*, *382*(6589), 363–366. https://doi.org/10.1038/382363a0

Moffat, J. J., Ka, M., Jung, E. M., & Kim, W. Y. (2015, November 5). Genes and brain malformations associated with abnormal neuron positioning. *Molecular Brain*, Vol. 8. https://doi.org/10.1186/s13041-015-0164-4

Nestor, S. M., Rupsingh, R., Borrie, M., Smith, M., Accomazzi, V., Wells, J. L., … Bartha, R. (2008). Ventricular enlargement as a possible measure of Alzheimer's disease progression validated using the Alzheimer's disease neuroimaging initiative database. *Brain*, *131*(9), 2443–2454. https://doi.org/10.1093/brain/awn146

Nopoulos, P., Flaum, M., O'leary, D., & Andreasen, N. C. (2000). Sexual dimorphism in the human brain: evaluation of tissue volume, tissue composition and surface anatomy using magnetic resonance imaging. In *Psychiatry Research: Neuroimaging Section* (Vol. 98).

O'Connor, E., Devesa, A., Garci´a, C., Puertes, I. R., Pelli´n, A., & Vin˜a, J. R. (1995). Biosynthesis and maintenance of GSH in primary astrocyte cultures: role ofl-cystine and ascorbate. *Brain Research*, *680*(1–2), 157–163. https://doi.org/10.1016/0006-8993(95)00257-Q

Ottestad-Hansen, S., Hu, Q. X., Follin-Arbelet, V. V., Bentea, E., Sato, H., Massie, A., … Danbolt, N. C. (2018). The cystine-glutamate exchanger (xCT, Slc7a11) is expressed in significant concentrations in a subpopulation of astrocytes in the mouse brain. *GLIA*, *66*(5), 951–970. https://doi.org/10.1002/glia.23294

Pfrieger, F. W., & Barres, B. A. (1997). Synaptic efficacy enhanced by glial cells in vitro. *Science*, *277*(5332), 1684–1687. https://doi.org/10.1126/science.277.5332.1684

Poldrack, R. A., Clark, J., Paré-Blagoev, E. J., Shohamy, D., Creso Moyano, J., Myers, C., & Gluck, M. A. (2001). Interactive memory systems in the human brain. *Nature*, *414*(6863), 546–550. https://doi.org/10.1038/35107080

Pow, D. V. (2001). Visualising the activity of the cystine-glutamate antiporter in glial cells using antibodies to aminoadipic acid, a selectively transported substrate. *Glia*, *34*(1), 27–38. https://doi.org/10.1002/glia.1037

Proescholdt, M. G., Hutto, B., Brady, L. S., & Herkenham, M. (2000). STUDIES OF CEREBROSPINAL FLUID FLOW AND PENETRATION INTO BRAIN FOLLOWING LATERAL VENTRICLE AND CISTERNA MAGNA INJECTIONS OF THE TRACER [14 C]INULIN IN RAT. *Neuroscience*, *95*(2), 577–592. Retrieved from www.elsevier.com/locate/neuroscience

Rahimi-Balaei, M., Bergen, H., Kong, J., & Marzban, H. (2018, December 17). Neuronal migration during development of the cerebellum. *Frontiers in Cellular Neuroscience*, Vol.

12, p. 484. https://doi.org/10.3389/fncel.2018.00484

Sato, H., Shiiya, A., Kimata, M., Maebara, K., Tamba, M., Sakakura, Y., … Bannai, S. (2005). *Redox Imbalance in Cystine/Glutamate Transporter-deficient Mice **. https://doi.org/10.1074/jbc.M506439200

Scharfman, H. E. (2007, July). The neurobiology of epilepsy. *Current Neurology and Neuroscience Reports*, Vol. 7, pp. 348–354. https://doi.org/10.1007/s11910-007-0053-z

Sears, S. M. S. (2018). Regulation of in vivo excitatory/inhibitory balance by the cystine/ glutamate exchanger system xc-. *Syracuse University SOURCE*.

Shih, A. Y., Erb, H., Sun, X., Toda, S., Kalivas, P. W., & Murphy, T. H. (2006). Cystine/glutamate exchange modulates glutathione supply for neuroprotection from oxidative stress and cell proliferation. *Journal of Neuroscience*, *26*(41), 10514–10523. https://doi.org/10.1523/JNEUROSCI.3178-06.2006

Sowell, E. R., Levitt, J., Thompson, P. M., Holmes, C. J., Blanton, R. E., David Kornsand, B. S., … Toga, A. W. (2000). Brain Abnormalities in Early-Onset Schizophrenia Spectrum Disorder Observed With Statistical Parametric Mapping of Structural Magnetic Resonance Images. In *Am J Psychiatry* (Vol. 157).

Vasile, F., Dossi, E., & Rouach, N. (2017, July 1). Human astrocytes: structure and functions in the healthy brain. *Brain Structure and Function*, Vol. 222, pp. 2017–2029. https://doi.org/10.1007/s00429-017-1383-5

Wang, X. F., & Cynader, M. S. (2002). Astrocytes Provide Cysteine to Neurons by Releasing Glutathione. *Journal of Neurochemistry*, *74*(4), 1434–1442. https://doi.org/10.1046/j.1471-4159.2000.0741434.x

Yager, L. M., Garcia, A. F., Wunsch, A. M., & Ferguson, S. M. (2015, July 4). The ins and outs of the striatum: Role in drug addiction. *Neuroscience*, Vol. 301, pp. 529–541. https://doi.org/10.1016/j.neuroscience.2015.06.033

Zhang, Y., Chen, K., Sloan, S. A., Bennett, M. L., Scholze, A. R., O'Keeffe, S., … Wu, J. Q. (2014). An RNA-sequencing transcriptome and splicing database of glia, neurons, and vascular cells of the cerebral cortex. *Journal of Neuroscience*, *34*(36), 11929–11947. https://doi.org/10.1523/JNEUROSCI.1860-14.2014